Interaction between Nitric Oxide and Ethylene in the Induction of Alternative Oxidase in Ozone-Treated Tobacco Plants[1][W]

Luisa Ederli, Roberta Morettini, Andrea Borgogni, Claus Wasternack, Otto Miersch, Lara Reale, Francesco Ferranti, Nicola Tosti[2], and Stefania Pasqualini*

Department of Plant Biology and Agro-Environmental and Animal Biotechnology, University of Perugia, I–06121 Perugia, Italy (L.E., R.M., A.B., L.R., F.F., S.P.); Leibniz-Institut für Pflanzenbiochemie, D–06120 Halle (Saale), Germany (C.W., O.M.); and Institute of Plant Genetics, Consiglio Nazionale delle Ricerche, I–06128, Perugia, Italy (N.T.)

The higher plant mitochondrial electron transport chain contains, in addition to the cytochrome chain, an alternative pathway that terminates with a single homodimeric protein, the alternative oxidase (AOX). We recorded temporary inhibition of cytochrome capacity respiration and activation of AOX pathway capacity in tobacco plants (*Nicotiana tabacum* L. cv BelW3) fumigated with ozone (O_3). The *AOX1a* gene was used as a molecular probe to investigate its regulation by signal molecules such as hydrogen peroxide, nitric oxide (NO), ethylene (ET), salicylic acid, and jasmonic acid (JA), all of them reported to be involved in the O_3 response. Fumigation leads to accumulation of hydrogen peroxide in mitochondria and early accumulation of NO in leaf tissues. Although ET accumulation was high in leaf tissues 5 h after the start of O_3 fumigation, it declined during the recovery period. There were no differences in the JA and 12-oxo-phytodienoic acid levels of treated and untreated plants. NO, JA, and ET induced AOX1a mRNA accumulation. Using pharmacological inhibition of ET and NO, we demonstrate that both NO- and ET-dependent pathways are required for O_3-induced up-regulation of *AOX1a*. However, only NO is indispensable for the activation of *AOX1a* gene expression.

Mitochondrial respiration provides the energy necessary to drive cellular metabolism and transport processes. Plant mitochondria possess two different pathways of electron transport at the ubiquinone level, the cyanide-sensitive cytochrome (cyt) pathway and the cyanide-resistant alternative pathway. A single enzyme, the alternative oxidase (AOX), is responsible for the latter. Electron transfer through the cyt pathway is coupled to the synthesis of ATP. Since the AOX catalyzes oxidation of reduced ubiquinone without forming an electrochemical gradient, it does not appear to be coupled to ATP synthesis (Vanlerberghe and McIntosh, 1997; McDonald et al., 2002). The AOX protein is found in every examined plant species and in almost every plant organ. The AOX proteins are encoded by a small gene family that has highly conserved regions (Whelan et al., 1996; Vanlerberghe and McIntosh, 1997). Taken together, these findings suggest that the alternative pathway plays a vital role in plant functioning. However, apart from its role in thermogenesis, the biological function of AOX is not fully understood. Its role is generally considered as allowing increased carbon flux through the tricarboxylic acid cycle when ADP supply limits cyt pathway activity and consequently providing carbon skeletons for other cellular processes (Lambers and Steingrover, 1978). Another possible function of the alternative pathway might be to reduce the formation of reactive oxygen species (ROS). The mitochondrial electron transport chain produces significant quantities of ROS, primarily due to the presence of the ubisemiquinone radical, which can transfer a single electron to oxygen, leading to the generation of superoxide (Halliwell and Gutteridge, 1999). The half-life of ubisemiquinone increases if the electron transport chain is overreduced. Consequently, mechanisms that increase or maintain the flow of electrons out of the ubiquinone pool may reduce ROS production. Enhanced activity of AOX could relieve the cyt pathway and prevent overreduction, reducing the formation of harmful radicals (Purvis and Shewfelt, 1993; Wagner and Krab, 1995).

ROS generation is thought to be involved in biotic and abiotic stresses in plants. While AOX abundance and AOX activity are low in unstressed plants, alternative respiration is enhanced after various developmental or environmental stimuli, especially in stress

[1] This work was supported by a grant from MIUR (National Project; COFIN 2005) and by a grant of Fondazione Cassa di Risparmio.

[2] Present address: &LAB Srl, Via Strozzacapponi, 89/a, I–06071 Perugia, Italy.

* Corresponding author; e-mail spas@unipg.it; fax 39–0755856404.

The author responsible for distribution of materials integral to the findings presented in this article in accordance with the policy described in the Instructions for Authors (www.plantphysiol.org) is: Stefania Pasqualini (spas@unipg.it).

[W] The online version of this article contains Web-only data.

www.plantphysiol.org/cgi/doi/10.1104/pp.106.085472

conditions, e.g. low temperature, wounding, and plant diseases (Purvis and Shewfelt, 1993). Alternative respiration therefore seems to be implicated in stress alleviation. The nuclear gene that encodes AOX in tobacco (*Nicotiana tabacum*; *AOX1*) is rapidly induced in cultured cells when the cyt pathway is specifically inhibited by antimycin A (Vanlerberghe and McIntosh, 1994). The AOX has been demonstrated to be an antioxidant enzyme in both bell pepper (*Capsicum annuum*) mitochondria (Purvis, 1997) and intact tobacco cells (Maxwell et al., 1999). In plants, regulation of AOX activity is complex and occurs both transcriptionally and posttranslationally. In mitochondria isolated from higher plants, AOX activity increases strongly upon reduction of an intersubunit disulfide bridge to yield a noncovalently linked dimeric protein. In its reduced form, the enzyme is activated by α-keto acids, including pyruvate (Affourtit et al., 2002). Under stress conditions, ROS levels may induce *AOX* expression (Vanlerberghe and McIntosh, 1996; Maxwell et al., 2002; Vanlerberghe et al., 2002). Addition of salicylic acid (SA) to tobacco cell suspensions or intact leaves also induces *AOX* gene expression (Rhoads and McIntosh, 1993; Lennon et al., 1997).

In recent years, nitric oxide (NO) has been identified as a fundamental molecule that interplays with ROS in a variety of ways, either as a crucial partner in determining cell fate or in signaling in response to a number of physiological and stress-related conditions. NO appears to be involved in controlling various aspects of plant pathogen resistance, growth, development, and senescence, as well as stomatal movement (Delledonne et al., 1998; Beligni and Lamattina, 2000; Garcia-Mata and Lamattina, 2002; Neill et al., 2002). NO may induce the AOX pathway by inhibiting cyt oxidase (Millar and Day, 1996). In Arabidopsis (*Arabidopsis thaliana*) cell cultures treated with NO, *AOX1a* expression is strongly induced, resulting in increased respiration through the alternative pathway (Huang et al., 2002). Furthermore, *AOX* expression is affected in the Arabidopsis *ctr-1* mutant, indicating ethylene (ET) dependence (Simons et al., 1999). Different signaling molecules have been found to be involved in *AOX* expression, but their interactions during environmental stresses are unclear. Analyses of Arabidopsis mutants have produced a large body of information implicating SA, NO, ROS, jasmonic acid (JA), and ET as major endogenous signals in defense responses. However, much less information is available for other plant species. Our previous studies demonstrated that ozone (O_3) treatment induces SA and hydrogen peroxide (H_2O_2) accumulation in the O_3-sensitive tobacco BelW3 cultivar (Pasqualini et al., 2002), and the activation of a cell death program (Pasqualini et al., 2003). Here, the induction of the AOX pathway by O_3 in BelW3 plants is reported. Early production of NO in fumigated leaves was detected with a NO-specific fluorescence. H_2O_2 accumulation in mitochondria and ET evolution was recorded during O_3 exposure. Moreover, whereas no significant increase in JA or its precursor cis-(+)-12-oxo-phytodienoic acid (OPDA) was found, some JA conjugates strongly increased after O_3 exposure. Our experiments suggest that in O_3-fumigated tobacco plants, NO is the preferred signaling molecule involved in *AOX* gene expression, which is coordinately activated by ET.

RESULTS

Inhibition of the Cyt Pathway and Activation of the Alternative Pathway by O_3

The BelW3 tobacco cultivar is particularly sensitive to O_3 (Heggestad, 1991). O_3 fumigation (150 nL L^{-1} O_3) for 5 h led to visible symptom development in mature and old leaves. After 48 h from the start of O_3 fumigation, we scored foliar lesions on about 30% of the fourth-leaf area.

Respiratory pathway capacities were determined in mitochondria isolated from unfumigated and O_3-fumigated plants. The cyt pathway capacity decreased by approximately 50% after 2.5 h of O_3 treatment (Fig. 1A). Although inhibition was partially reversed during the recovery period, cyt capacity never reached the levels measured in unfumigated plants. The decrease in the cyt capacity was accompanied by a significant induction of AOX capacity in mitochondria. AOX capacity started to increase after 5 h and reached a maximum at 10 h after the onset of fumigation (Fig. 1B). The cyt pathway declined during ozonization before AOX capacity increased. Consequently, the total respiration rate was considerably inhibited during the fumigation (Fig. 1C) and did not completely recover until 10 h after the onset of fumigation.

O_3 Up-Regulated *AOX* Expression But Decreased Cyt *c* Protein Content

Levels of mRNAs of *AOX*, *COXI*, and *COXII* genes were assessed following treatment with 150 nL L^{-1} O_3 for 5 h (Fig. 2). Increased AOX1a accumulation was evident 1.5 h after the onset of fumigation, peaking at the end of fumigation (5 h) and decreasing to control levels during the recovery time (10 h). In contrast, AOX2 mRNA content accumulated much less than AOX1a mRNA and peaked at 10 h, followed by a decline to control levels. Levels of mitochondrial COXI and COXII mRNAs were not affected by O_3 fumigation.

Levels of different proteins were measured in both O_3-treated and untreated BelW3 tobacco plants. The AOX protein was constitutively detectable, thus corresponding to the constitutive AOX capacity (Fig. 1B versus Fig. 3). After treatment with 150 nL L^{-1} of O_3, however, the AOX protein level increased, peaking at 5 h, and then decreased (Fig. 3). Immunoblot analysis for COXI and COXII revealed no change in mitochondria isolated from either treated or untreated plants. In contrast, the cyt *c* protein level declined from 1.5 h to 2.5 h from the start of fumigation, then increased to the control level (Fig. 3). To evaluate whether mitochondrial

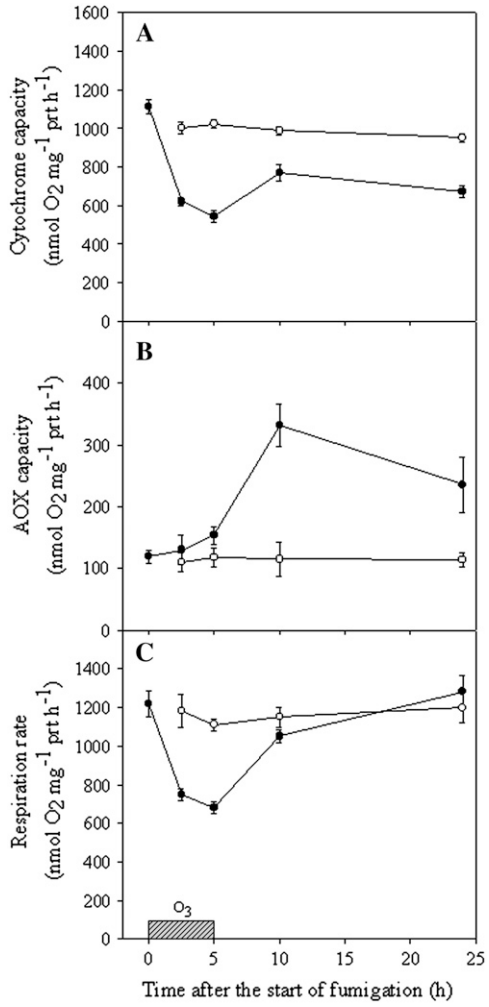

Figure 1. Measurements of respiratory pathway capacities in mitochondria from BelW3 plants treated with 150 nL L^{-1} O_3 for 5 h. A, Cyt capacity detected in mitochondria purified from unfumigated (white circles) and O_3-treated plants (black circles), sampled before and at different times (2.5, 5, 10, and 24 h) after the start of fumigation. Cyt capacity is defined as O_2 uptake that was sensitive to 3 mM KCN in the presence of 1 mM SHAM. B, AOX capacity in unfumigated plants (white circles) and fumigated plants (black circles). AOX capacity is defined as the O_2 uptake that was sensitive to 1 mM SHAM in the presence of 3 mM KCN. C, Respiration rate in unfumigated plants (white circles) and in fumigated plants (black circles). Respiration rate refers to O_2 uptake in the absence of any addition. Data are the mean ± SE from four independent experiments.

cyt *c* was released into the cytosol, the cytosolic fraction was probed for cyt *c*. In this fraction a slight increase of cyt *c* was detectable during O_3 treatment, indicating that the cyt *c* was at least partially released into the cytosol, which would allow impairment of the cyt respiratory pathway.

H_2O_2 Accumulated in Mitochondria from Fumigated Leaves

To determine whether the O_3 fumigation induced ROS accumulation in mitochondria, H_2O_2 was measured spectrophotometrically in isolated mitochondria from control and O_3-treated plants (Fig. 4). As H_2O_2 was barely detectable in mitochondria from unfumigated plants, the isolation procedure did not generate H_2O_2. O_3 exposure triggered a marked increase in H_2O_2, which peaked 2.5 h after onset of fumigation.

Induction of *AOX1a* Expression by Different Elicitors

Different chemical elicitors were tested to determine whether any of them induced *AOX* expression in BelW3 tobacco plants. Figure 5 shows AOX1a mRNA level after elicitation with H_2O_2, SA, the NO chemical donor sodium nitroprusside (SNP), JA, and ET. There was no significant induction of AOX1a mRNA after infiltration of leaf discs with H_2O_2 and SA. In contrast, treatment with SNP, JA, and ET strongly induced AOX1a transcript content. It is well documented that both NO and cyanide can be released from SNP decomposition (Bentke et al., 2006). Since cyanide has been reported to transcriptionally activate *AOX* gene in tobacco (Sabar et al., 2000) and maize (*Zea mays*; Polidoros et al., 2005), we infiltrated leaf discs with ferrocyanide to exclude the possibility that the observed induction of *AOX1a* could be due to an overlapping of NO and cyanide. Furthermore, to determine the specificity of the NO signal, we simultaneously infiltrated leaf discs with SNP and 2-(4-carboxyphenyl)-4,4,5,5-tetramethylimidazoline-1-oxyl-3-oxide (cPTIO), a NO scavenger. Figure 5 shows that 160 μM ferrocyanide, as expected, strongly induced *AOX1a*. However, the evidence that SNP plus cPTIO completely reversed the *AOX1a* induction leads us to conclude that (1) *AOX1a* induction can be ascribed exclusively to NO and (2) cyanide was not released after 2 h in SNP-treated leaf discs. The latter is confirmed by the fact that cyanide was undetectable after 2 h in SNP-treated leaf discs. In fact, the cyanide was released from SNP in a time-dependent manner and a significant cyanide concentration was detected starting from 5 h of incubation (Supplemental Fig. S1).

NO Accumulated under O_3 Stress

Because the application of exogenous NO affected *AOX* gene expression, it was important to know whether ozonated tobacco plants themselves produced NO. The fluorescent probe 4-amino-5-methylamino-2′,7′-difluorofluorescein diacetate (DAF-FM diacetate) is highly specific for NO and does not react with other ROS (Kojima et al., 1998). Since the green fluorescence detected with the UV epifluorescence microscope disappeared following addition of 100 μM cPTIO, the visual signal can be ascribed to NO accumulation (not shown). In unfumigated plants, apart from the time of sampling, fluorescence was very low or undetectable (Fig. 6A). Exposure to O_3 resulted in a rapid burst of fluorescence that indicates massive NO production. NO production significantly increased after 1 h (Fig. 6B), peaked at 1.5 h (Fig. 6C), and then

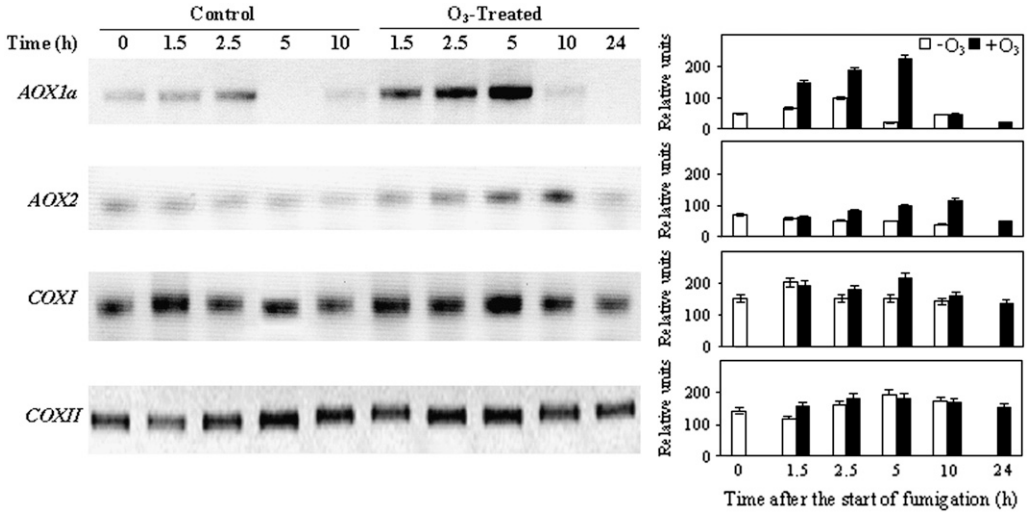

Figure 2. Semiquantitative RT-PCR for *AOX1a*, *AOX2*, *COXI*, and *COXII* genes from unfumigated and O_3-treated plants. Tobacco plants were treated with 150 nL L^{-1} O_3 for 5 h and sampled after 1.5, 2.5, and 5 h of fumigation and, during the recovery time, after 10 and 24 h from starting fumigation. Total RNA (1–2 μg) was reverse transcribed and amplified by RT-PCR. Semiquantitation of mRNA levels loaded in each lane was performed by coamplification and normalization with an internal standard (actin). Beside each blot, a graph with relative intensities of the signals ± SE is shown.

decreased after 2 h (Fig. 6D). Fluorescence was visible in the chloroplasts of palisade cells (Fig. 6C). Figure 6G shows the time course of DAF-FM fluorescence measured as a percentage of fluorescent cells from O_3-treated leaves compared with that detected in unfumigated control plants. The fact that NO reached its highest accumulation after 1.5 h from the onset of fumigation suggests that NO is an early signal molecule produced in response to O_3 in BelW3 plants. NO accumulation time course was similar in ET-inhibited plants [(*S*)-Trans-2-amino-4-(2-aminoethoxy)-3-butenoic acid hydrochloride, or AVG; Fig. 6G]. On the contrary, NO failed to accumulate in NO-inhibited plants (+cPTIO-L-nitro-L-Arg [LNNA]) subjected to O_3 fumigation (Fig. 6, E–G).

JA Failed to Accumulate in Ozonated Tobacco Plants

As *AOX1a* was strongly induced by JA in tobacco leaf discs, jasmonate accumulation was assessed in BelW3 leaves after acute O_3 fumigation. Although O_3-induced increase in JA levels has been documented in Arabidopsis (Rao et al., 2000; Tuominen et al., 2004) and poplar (*Populus* spp.; Koch et al., 2000), there is, to our knowledge, no evidence that JA is implicated in the response of tobacco plant to O_3. Örvar et al. (1997) reported that O_3 injury was markedly reduced in BelW3 plants treated with methyl jasmonate (JAME) prior to challenge with O_3, suggesting responsiveness and protection by JA in BelW3 plants. However, Örvar et al. (1997) did not measure JA content in BelW3-fumigated plants. We monitored JA levels in control and fumigated plants, but detected no significant increase in JA at any time point considered (two-way ANOVA; unfumigated/fumigated and time as factors; $P = 0.402$; see Supplemental Fig. S2A). However, this does not exclude a rapid and transient increase in JA synthesis early in the response of BelW3 plants to O_3. To ascertain whether this occurred, tissues were harvested 20, 40, 60, and 90 min after the start of fumigation. Again, no increase in JA content was detected (two-way ANOVA; unfumigated/fumigated and time

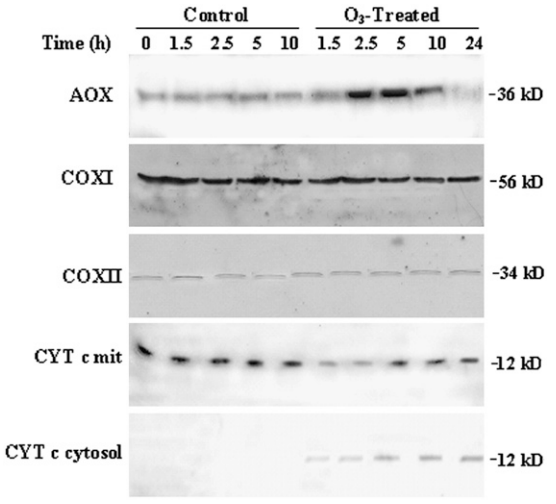

Figure 3. Immunoblot analysis of AOX, COXI, COXII, and cyt *c* from unfumigated (control) and O_3-treated plants. Tobacco plants were treated with 150 nL L^{-1} O_3 for 5 h and sampled after 1.5, 2.5, and 5 h of fumigation and, during the recovery time, after 10 and 24 h from starting fumigation. Leaf mitochondria were isolated, and mitochondrial (20–150 μg) and cytosolic (100 μg) proteins were used for immunoblot analysis. Proteins were detected using specific antibodies combined with a chemiluminescence detection system. Numbers on the right of the image indicate approximate molecular mass in kD. Representative results are shown.

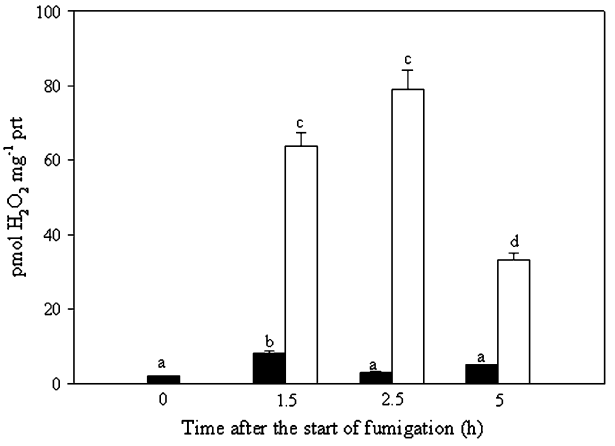

Figure 4. H_2O_2 accumulation in purified mitochondria from unfumigated (black bars) and fumigated (white bars) plants. The data are the mean ± SE from four independent experiments. Bars showing the same letter are not significantly different ($P \leq 0.01$ as ANOVA test).

as factors; $P = 0.980$; Supplemental Fig. S2, inset a). We also quantified OPDA, a precursor of JA shown to be active in pathogen infection, but failed to reveal any change during or after acute O_3 fumigation (two-way ANOVA; unfumigated/fumigated and time as factors; $P = 0.343$ and $P = 0.798$ for B and inset b, respectively, in Supplemental Fig. S2). When the JA derivatives 11-hydroxyjasmonic acid, JAME, and Ile jasmonic acid were searched for, they were below the detection limit. Interestingly, we detected after 24 h from the start of O_3 fumigation a significant increase in both sulfated (12-HSO_4-JA) and glucosyl JA (12-*O*-Gluc-JA; Supplemental Fig. S2C), suggesting that in BelW3 tobacco plants JA was rapidly metabolized.

NO Induced ET Evolution, But ET Did Not Induce NO

The effect of NO on ET accumulation was determined in leaf discs and in planta. By infiltrating leaf discs with different concentrations of the NO donor SNP, we found that ET evolution was very high after 1.5 h of infiltration with 1 mM SNP and that it was SNP concentration dependent (Fig. 7A). The NO donor also enhanced mRNA accumulation of the ET biosynthetic gene *ACS2* (Fig. 7E), indicating that NO potentiates ET production by inducing a gene of its biosynthesis. The lack of *ACS2* gene induction after infiltration with the SNP analog ferrocyanide and with SNP plus cPTIO demonstrates that NO but not cyanide specifically induced the ET biosynthetic gene. To investigate the effect of NO on the induction of cell death, leaf discs were incubated in the presence of the NO donor SNP and the incorporation of Evans blue evaluated. The data of Figure 7C show that cell death started to increase significantly at 8 h and continued to increase until 24 h after SNP application. When leaf discs were treated with the inhibitor of ET synthesis AVG plus SNP, no significant increase in cell death was observed (Fig. 7C). To evaluate the role of NO on ET evolution in planta, NO accumulation was suppressed and ET evolution measured. NO was suppressed by pretreating tobacco plants with the NO scavenger cPTIO prior to fumigation. LNNA, *N*-monomethyl-L-Arg, and *N*-nitro-Arg-methyl ester, which are inhibitors of a mammalian type of NO synthase (NOS), are active in several plant species (Delledonne et al., 1998). We therefore used LNNA plus cPTIO to abolish NO accumulation in fumigated tobacco leaves. The coapplication of cPTIO and LNNA did not significantly influence O_3 uptake by the leaf compared with water-treated plants (Fig. 7D). O_3 treatment exerted significant effects on ET production in BelW3 plants. ET evolution increased within 2 h of starting treatment, reached a maximum at 5 h, and then decreased to near control value (Fig. 7B). When NO accumulation was blocked (+cPTIO-LNNA), as confirmed by fluorescence analysis (Fig. 6, E–G), there was a dramatic reduction in ET production (Fig. 7B) and O_3-induced visual damage on the leaves was greatly reduced (5%). There was no increase in transcript amount of *ACS2* in fumigated plants pretreated with cPTIO-LNNA (Fig. 7F).

To investigate whether ET induced NO accumulation, BelW3 free-hand sections sampled from ET-treated

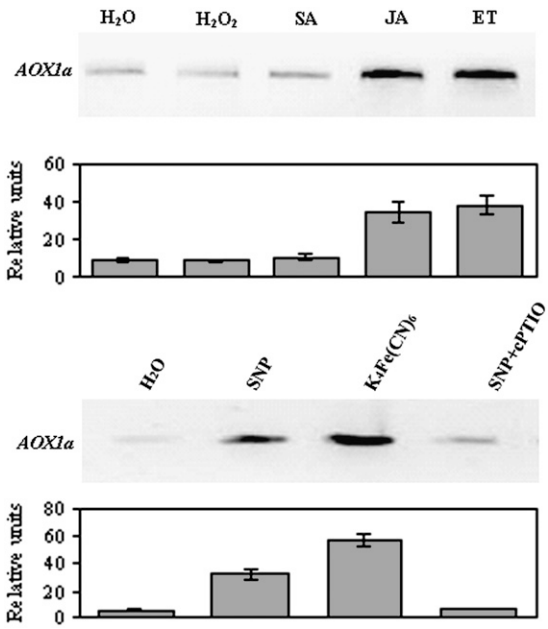

Figure 5. Analysis of the expression pattern of *AOX1a* gene after addition of different elicitors. Leaf discs were infiltrated for 3 min with the following compounds: 5 mM H_2O_2, 1 mM SA, 100 μM JA, and ET (top). ET treatment of plants was performed in a plexiglass chamber. A volume of ET was injected into the chamber to give a final concentration of 10 μL L^{-1}. Bottom shows expression pattern of *AOX1a* gene after infiltration with 160 μM SNP, 160 μM ferrocyanide, 160 μM SNP plus 200 μM cPTIO, and water as control. Semiquantitation of mRNA levels loaded in each lane was performed by coamplification and normalization with an internal standard (actin). Under the blot, a graph with relative intensities of the signals ± SE is shown.

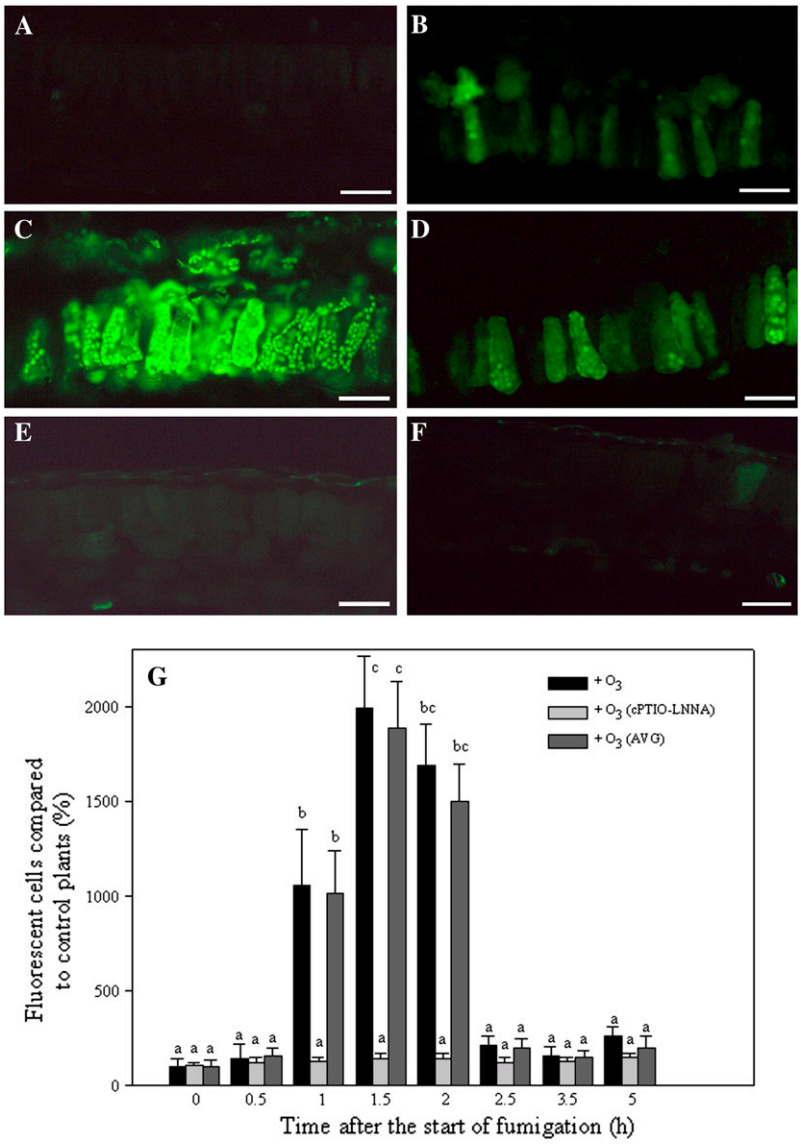

Figure 6. NO visualization in mesophyll cells from control and ozonated BelW3 plants. A, Section from unfumigated plants sampled immediately before the start of O_3 fumigation. B to D, Sections from leaf tissue fumigated with 150 nL L^{-1} O_3 and sampled after 1, 1.5, and 2.0 h from the start of fumigation, respectively. E and F, Sections from leaf tissue fumigated with 150 nL L^{-1} O_3 and sampled after 1.5 (E) and 2.0 h (F) from the start of fumigation. Plants were treated with cPTIO and LNNA to quench NO. Sections were loaded with DAF-FM diacetate and then examined with a fluorescence microscope. Bar = 35 μm. G, Time course of percentage of fluorescent cells detected in ozonated plants and in ozonated plants pretreated with AVG or cPTIO/LNNA compared with the fluorescent cells counted in control sections (time 0) and done as 100. Data are the mean ± SE from four independent experiments. Bars showing the same letter are not significantly different ($P \leq 0.05$ as ANOVA test).

plants (10 μL L^{-1} for 2 h) were incubated with the NO probe DAF-FM. No NO accumulation was detected in these sections (data not shown).

O_3-Induced *AOX* Induction Is Reversed by Inhibition of NO and ET

Although, potentially, JA could be implicated in activating AOX (Fig. 5), the fact that it does not accumulate during O_3 fumigation in BelW3 plants suggests that it is not involved in *AOX* activation in planta. Therefore, the two candidate signal molecules that accumulate early during O_3 fumigation and are compatible with the times of *AOX* activation are NO and ET. O_3 induces NO (Fig. 6) and ET accumulation (Fig. 7B), which, in turn, both lead to accumulation of AOX1a transcript (Fig. 5). To test whether NO and ET are involved in O_3-induced AOX mRNA accumulation, we suppressed ET production by painting the leaves, prior to fumigation, with the ET synthesis inhibitor AVG and suppressed NO accumulation by pretreating plants with cPTIO plus LNNA. Treatment with AVG, an inhibitor of 1-aminocyclopropane-1-carboxylic acid synthase, completely abolished O_3-induced ET evolution (Fig. 7B). Pretreatment of tobacco plants with AVG did not induce significant differences in the O_3 uptake by the leaf with respect to AVG-untreated plants (data not shown). However, treatment with AVG greatly reduced foliar injury in ozonated leaves (2%). As previously mentioned, NO accumulated in ozonated AVG-treated plants (Fig. 6G) but was completely abolished in cPTIO-LNNA-treated plants (Fig. 6, E–G). AOX1a mRNA accumulation was completely abolished in NO-inhibited plants (+cPTIO-LNNA) and was partially reversed in ET-inhibited plants (+AVG), indicating that both NO and ET are required for *AOX* induction, but only NO is indispensable for *AOX* induction (Fig. 8).

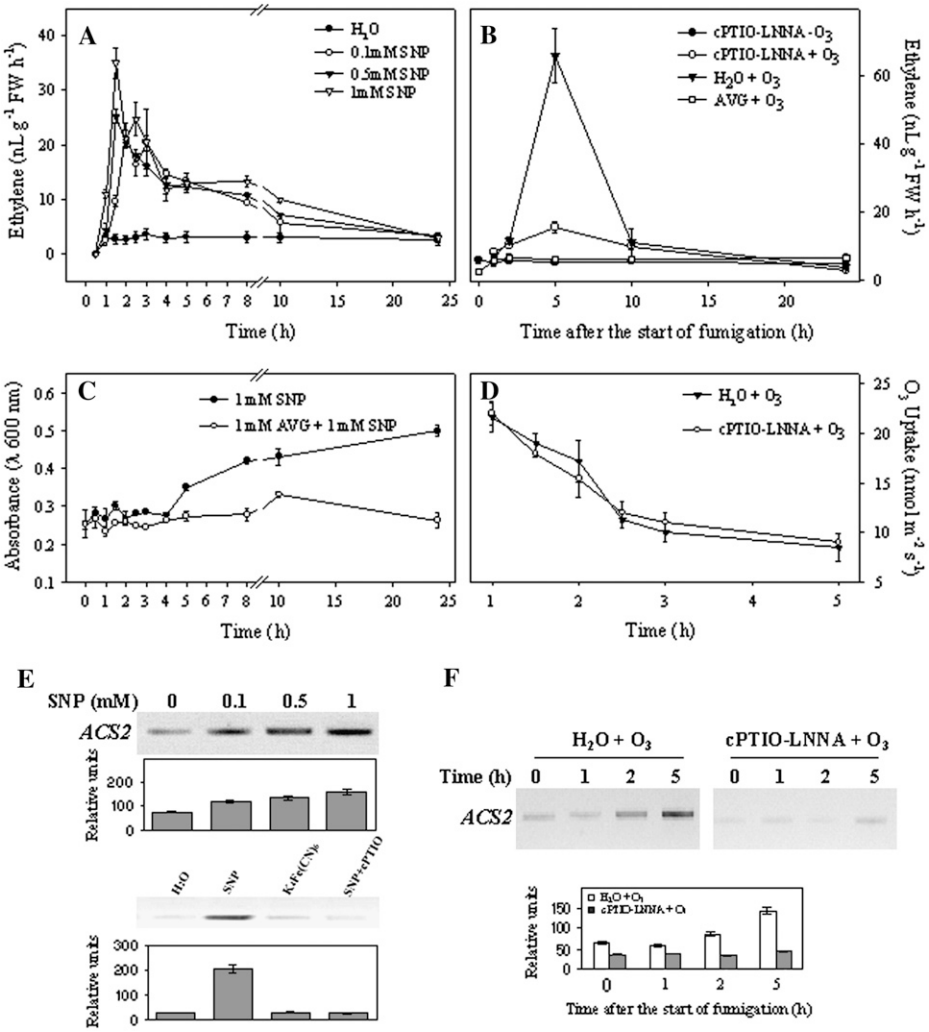

Figure 7. ET emission and expression profile of *ACS2* from leaf pieces after infiltration with the NO donor SNP or after inhibition of NO by cPTIO-LNNA and ET by AVG. A, ET emission from leaf pieces infiltrated for 3 min with different SNP concentrations (0.1, 0.5, and 1 mM) and analyzed after 0.5, 1, 1.5, 2, 2.5, 3, 4, 5, 8, 10, and 24 h. The control was infiltrated with distilled water. The data are the mean of four different experiments ± SE. B, ET emission from NO-inhibited by cPTIO-LNNA and ET-inhibited plants by AVG application and subjected to O_3 fumigation. Control plants were painted with water and then fumigated. Results are the average of four different experiments ± SE. C, Time course of cell death estimated by Evans blue staining in leaf pieces infiltrated with 1 mM SNP or with 1 mM AVG plus 1 mM SNP and analyzed at the time points reported in A. The data are the mean of four different experiments ± SE. D, Time course of O_3 uptake during 5-h O_3 fumigation in plants painted with water before the fumigation or painted with cPTIO-LNNA. Results show the average of four different experiments ± SE. E, ACS2 mRNA expression detected 1 h after infiltration of leaf pieces with 0.1, 0.5, and 1 mM of SNP (top), and 1 mM SNP, 1 mM ferrocyanide, and 1 mM SNP plus 1 mM cPTIO (bottom). Total RNA (1–2 μg) was reverse transcribed and amplified by RT-PCR. mRNA levels loaded in each lane were determined by coamplification and normalization with an internal standard (actin). Close to the blots, graphs with relative intensities of the signals ± SE were shown. F, RNA expression of the *ACS2* gene from samples taken from plants painted with water or with cPTIO-LNNA and then O_3 fumigated. Total RNA (1–2 μg) was reverse transcribed and amplified by RT-PCR. Semiquantitation of mRNA levels loaded in each lane was performed by coamplification and normalization with an internal standard (actin). Close to the blot, a graph with relative intensities of the signals ± SE is shown.

DISCUSSION

O_3 Reversibly Inhibits Cyt Respiration But Activates the Mitochondrial Alternative Pathway

The role of plant mitochondria in cell death and stress resistance is of increasing interest (Jones, 2000; Lam et al., 2001). We previously demonstrated that mitochondria are crucially implicated in O_3-triggered programmed cell death (PCD), as suggested by the coordinate caspase-like activation through the release of cyt *c* into the cytosol (Pasqualini et al., 2003). In this research we investigated mitochondrial activities during and after acute O_3 fumigation by analyzing both the cyt and the alternative pathways. Fumigation of

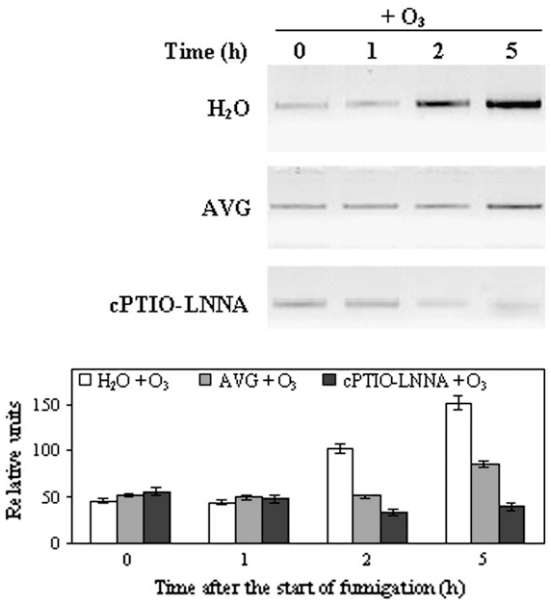

Figure 8. Changes in levels of the AOX1a transcript from O_3-fumigated plants after treatment with the ET inhibitor AVG or with the NO scavenger cPTIO and the NOS inhibitor LNNA. Twenty-four hours before the start of O_3 fumigation, tobacco leaves were painted on the adaxial surface with 1 mM AVG or 10 mM LNNA. Leaves pretreated with LNNA, 1.5 h before starting fumigation, were again painted with 200 μM cPTIO. This treatment was repeated three times during the fumigation. Control plants were brushed with distilled water. Sampling for mRNA analysis was done before and after 1, 2, and 5 h after the start of O_3 fumigation. Total RNA (1–2 μg) was reverse transcribed and amplified by RT-PCR. Under the blots, a graph with relative intensities of the signals ± SE is shown.

BelW3 plants with 150 nL L^{-1} O_3 for 5 h caused a drastic loss of the mitochondrial cyt pathway capacity during treatment. This is associated with marked induction of AOX at both activity and expression levels. Fumigation also triggered a rapid release of cyt *c* into the cytosol. Loss of cyt *c* from the inner mitochondrial membrane has been considered a crucial regulatory step in apoptosis (Kroemer, 1997). Recently, the involvement of PCD in O_3 lesion formation also has been reported in Arabidopsis plants (Overmyer et al., 2005). The severe loss of respiratory capacity induced by O_3 fumigation might be provoked by the release of cyt *c* from mitochondria and inhibition of COX activity. COX is thought to be the primary target of NO in the respiratory chain of both animal and plant mitochondria (Millar and Day, 1997). NO that accumulated in mesophyll cells during the O_3 fumigation could temporarily inhibit COX activity. To assess the NO-induced inhibition of respiratory capacities, we measured cyt and AOX capacities after addition of the NO donor SNP. We found that NO strongly lowered the cyt pathway, whereas it did not influence AOX capacity (Supplemental Fig. S3). The specificity of NO effect on respiratory capacities was confirmed by the recovery measured when SNP + cPTIO was added to the mixture assay (Supplemental Fig. S3). Inhibition of COX activity may increase electron flow from ubiquinone toward oxygen, thus stimulating superoxide and H_2O_2 formation. When the cyt pathway is directly inhibited by naturally occurring cyanide, NO, sulfide, high concentrations of CO_2, low temperature, or severely limiting phosphorus concentrations, electron transport is shunted into the alternative pathway (Millenaar and Lambers, 2003). Disruption of the cyt pathway leads to AOX induction in many organisms. For example, addition of antimycin A, a compound that blocks electron transport downstream of the ubiquinone pool, to cultured tobacco cells causes the induction of both AOX mRNA (Vanlerberghe and McIntosh, 1994) and AOX protein (Vanlerberghe et al., 1997). In nonthermogenic plants, AOX is thought to assist in minimizing the production of ROS by the respiratory chain (Vanlerberghe and McIntosh, 1997; Maxwell et al., 1999; Yip and Vanlerberghe, 2001). AOX is frequently induced during plant-pathogen interactions and plant defense and seems to be involved in both the containment of lesions and the control the initial plant defense reactions (Lennon et al., 1997; Chivasa and Carr, 1998). In addition, abiotic stress, such as cold (Atkin et al., 2002), markedly activates the alternative pathway. *AOX* gene induction has also been reported in the tobacco mutant CMSII, which is impaired in mitochondrial complex I function after severe O_3 stress (Dutilleul et al., 2003), and documented in O_3-treated Arabidopsis plants by microarray expression profiling (Tuominen et al., 2004; Tosti et al., 2006). Under O_3 treatment, we documented a marked rise in AOX capacity along with an enhanced *AOX1a* gene expression and AOX protein level. However, it should be stated that the high AOX capacity measured in isolated mitochondria after 10 h (Fig. 1B) corresponds with the low protein amount detected at the same time (Fig. 3). In the literature there is also no clear relationship between AOX concentration and AOX activity. Very often, high levels of protein do not correspond to similarly high AOX activity (Lennon et al., 1997; Millenaar et al., 2001). Further studies are needed to better understand the regulation of AOX functionality under O_3 stress.

O_3-Induced Impairment of Mitochondrial Functionality Leads to an Increase in H_2O_2

Generation of ROS by the mitochondrial respiratory chain is a physiological and continuous process that leads to a single electron reduction of up to 2% of the consumed oxygen in unstressed cells (Braidot et al., 1999). In addition, the inhibition of the respiratory electron transport chain can lead to production of ROS through the build up of singly reduced electron carriers that are subsequently oxidized by molecular oxygen. Under physiological conditions, the toxic effects of ROS are removed by antioxidant systems. However, under biotic and abiotic stresses, ROS concentration can rise significantly and reach a threshold that triggers

PCD. Our results show that O_3 can lead to the accumulation of H_2O_2 in mitochondria. The cyt respiration pathway was severely impaired during O_3 fumigation. At this time, the alternative pathway had not yet started to increase and it did not reach its maximum activity until 10 h from the start of fumigation. Therefore, the marked inhibition of cyt respiration during fumigation can lead to an increase in ROS. Our spectrophotometric analyses showed that H_2O_2 accumulated in ozonated mitochondria from 1.5 to 2.5 h after the start of fumigation, when the largest inhibition of the cyt respiration pathway was recorded. Acute ozonization is known to trigger apoplastic production of H_2O_2 in BelW3 plants (Schraudner et al., 1998; Pasqualini et al., 2002, 2003), but here we demonstrate that O_3 also induces H_2O_2 accumulation in mitochondria. However, with our methodological approach, we are not able to demonstrate if O_3-induced mitochondrial H_2O_2 can be due exclusively to the temporary impairment of cyt pathway. It is possible that the H_2O_2 we detected in mitochondria during O_3 fumigation could in part derive from a spreading of H_2O_2 from the apoplast into mitochondria.

Regulation of *AOX* Gene Expression: Which Signaling Molecules Potentially Stimulate Expression?

Of the several endogenous molecules proposed as signals in the response of plants to O_3, ROS (Rao and Davis, 2001; Pasqualini et al., 2003), SA (Sharma et al., 1996; Rao and Davis, 1999; Pasqualini et al., 2002), JA (Örvar et al., 1997; Tuominen et al., 2004), and ET (Tuomainen et al., 1997) are considered the major regulators of plant defense responses. Their role in signaling and in O_3-induced cell death has recently been reviewed by Kangasjärvi et al. (2005). Further, NO has been identified as a second messenger during the hypersensitive response to incompatible pathogens (Delledonne et al., 1998; Durner et al., 1998; Klessig et al., 2000), as well as to several abiotic stresses (Gould et al., 2003).

We were interested in discovering the signaling molecules required for the expression of *AOX1a*. It has been suggested that ROS is a component of AOX signaling (Minagawa et al., 1992; Vanlerberghe et al., 1998). Because treatment with the cyt pathway inhibitor antimycin A strongly induces AOX1 mRNA and AOX capacity in tobacco cells (Vanlerberghe and McIntosh, 1994) and generates substantial levels of ROS (Maxwell et al., 1999, 2002), oxidative stress would seem to be implicated. Besides antimycin A, H_2O_2 treatment also is reported to increase AOX mRNA abundance (Vanlerberghe and McIntosh, 1996; Maxwell et al., 2002). However, when BelW3 leaf discs were infiltrated with H_2O_2, no *AOX1a* gene induction was observed. A possible explanation is that H_2O_2 treatment could be ineffective, owing to the activation of H_2O_2-scavenging systems. To exclude this, we measured H_2O_2 in leaf discs after infiltration with 5 mM H_2O_2. After 2 h from infiltration, we detected a H_2O_2 concentration of 0.1 mM (see Supplemental Fig. S4). The different results could be due to the different experimental systems: Both in Vanlerberghe and McIntosh (1996) and in Maxwell et al. (2002), cell cultures were used and the increased *AOX* expression was found after 4 h of H_2O_2 treatment. Nevertheless, the fact that H_2O_2 did not induce *AOX1a* in BelW3 leaf discs does not exclude in planta mitochondrial H_2O_2 could being involved in induction of *AOX* expression during O_3 stress.

SA is an uncoupler and inhibitor of mitochondrial electron transport (Vanlerberghe and McIntosh, 1996; Maxwell et al., 2002; Norman et al., 2004). Although SA has been demonstrated to induce *AOX* expression (Rhoads and McIntosh, 1993; Norman et al., 2004), it does not appear to be involved in the O_3-induced *AOX1a* expression of BelW3 plants. The lack of *AOX* gene induction by SA could be due to the relatively short time of incubation with SA (2 h) used in our experiment, despite prolonged exposure reported to induce *AOX* expression (Norman et al., 2004; Polidoros et al., 2005). SA accumulated in ozonated BelW3 plants and peaked 7 h after the start of fumigation (Pasqualini et al., 2002), which is not compatible with the increased AOX1a transcripts being detectable as early as 1.5 h of fumigation.

JAME strongly increases steady-state AOX transcript levels in sweet peppers and reduces the incidence of chilling injury (Fung et al., 2004). JA markedly induced *AOX* expression in BelW3 leaf discs, but, as there was no significant increase in JA and JA derivative content during the O_3 exposure, JAs do not seem to be involved in *AOX* induction in BelW3 plants. Interestingly, we found a late increase in the content of sulfate and glucosyl JA conjugates. It has been reported that the metabolism of JA to 12-hydroxyjasmonic acid sulfate might be a route leading to its inactivation (Gidda et al., 2003). JA limits lesion spread by antagonizing ET and SA, which are responsible for the development of visible O_3-induced lesions (Overmyer et al., 2003; Tuominen et al., 2004). The extensive cell death we observed in BelW3 after acute O_3 fumigation was, therefore, attributable, concomitantly with the high ET and SA (Pasqualini et al., 2002), to a lack of JA pathway stimulation by O_3.

AOX activation also appears to be ET dependent in Arabidopsis ET-insensitive mutant (*ein2*; Tuominen et al., 2004) and in a mutant that has defective ET perception (*etr-1*; Simons et al., 1999). We show that ET boosts AOX mRNA content in tobacco leaf discs. O_3 rapidly induces ET formation in BelW3 plants, in agreement with the findings of Langebartels et al. (1991). To test whether O_3-induced *AOX1a* expression could be reversed when O_3-induced ET was inhibited, the steady-state AOX1a mRNA level was monitored in plants pretreated with AVG. Although induction still occurred, it was less pronounced than in ozonated plants pretreated with water, which suggests that both ET-dependent and ET-independent pathways are required for *AOX* expression.

Microarray experiments with Arabidopsis have revealed that NO up-regulates 342 genes, including *AOX1a* (Parani et al., 2004). Interestingly, NO also induces two ET biosynthetic genes: *ACO* and *ACS* (Huang et al., 2002; Parani et al., 2004). We recently reported that O_3 induces NO accumulation in the mesophyll cells of *Phragmites australis* leaves when isoprene emission was inhibited (Velikova et al., 2005). By monitoring NO production with a DAF-FM fluorophore, we demonstrated that NO accumulates early in tobacco mesophyll cells and peaks 1.5 h from the start of O_3 fumigation, thus showing compatibility with the *AOX* gene expression induction that we found in tobacco plants. As we failed to detect either NO accumulation or O_3-induced *AOX* up-regulation in plants treated with the NO quencher cPTIO and the NOS inhibitor LNNA, NO appears to be essential for *AOX* induction. Overall, our results suggest that O_3-induced *AOX* up-regulation was dependent on NO generation and ET biosynthesis and that NO and ET accumulation were two upstream signaling events essential for the O_3-induced *AOX* activation. Final proof can only be obtained by transgenic approaches or the use of signaling mutants, as done for Arabidopsis; however, these approaches are not yet available for tobacco.

Interaction between NO and ET Signaling Molecules

Using the NO donor SNP, we demonstrated that NO boosted ET accumulation in leaf discs and up-regulated ACS2 transcript levels. In addition, when ozonated plants were treated with the NO quencher cPTIO and the NOS inhibitor LNNA, no ET emission was detected and *ACS2* gene induction was completely reversed. However, when plants were treated for 2 h with ET, fluorescence analysis failed to reveal any NO accumulation. On the basis of these findings, we conclude that ET accumulation was dependent on NO generation, whereas ET did not induce NO emission. As ET accumulated subsequent to NO emission in ozonated plants, NO evolution appears to be ET independent. This conclusion gains further support from the finding that NO emission in AVG-treated and ozonated plants was similar to that recorded in ET-evolving plants. The NO donor SNP is known to induce cell death (Clarke et al., 2000; Zottini et al., 2002). Although early ET evolution and cell death have been shown to be correlated (Overmyer et al., 2003), it is not clear whether the induction of ET biosynthesis is a result of early cell death or, conversely, whether early cell death is a result of ET accumulation. To test whether the ET evolution we documented in SNP-treated leaf discs was directly induced by NO, we monitored the time course of cell death in NO-treated leaf discs. As ET evolution preceded cell death by several hours, we conclude that ET evolution is induced by NO and that it is not induced by cell death. This is also supported by the evidence that in leaf discs incubated with AVG and SNP together or in tobacco plants pretreated with AVG prior to fumigation, we did not measure cell death (Fig. 8C) or leaf damage, strengthening the conclusion that NO-induced ET is required for cell death. However, in the sequence of events triggered by O_3, the role of ROS should also be mentioned. Joo et al. (2005) recently reported that in Arabidopsis intracellular ROS production is an early response to O_3 stress. It remains to be elucidated how ROS interplay with NO and ET in the signaling pathway leads to cell death.

Mitochondrial Regulation of the Nuclear *AOX* Gene

Intercellular ROS are considered to be a cellular signal that may alter gene expression. The early accumulation of H_2O_2 content we documented in mitochondria should be added to that recorded in apoplast (Pasqualini et al., 2002, 2003). Mitochondrial ROS could connect mitochondria to the nuclei and therefore cause what is known as mitochondrial regulation of nuclear gene expression, found in plants as in other eukaryotes (Liao and Butow, 1993; Vanlerberghe and McIntosh, 1994; Poyton and McEwen, 1996; Djajanegara et al., 2002). O_3-induced mitochondrial ROS could be the result of a cyt pathway impairment caused by NO inhibition of COX. However, as the H_2O_2 that arose from cyt pathway inhibition by NO was the signaling molecule involved in induction of the nuclear *AOX* gene, NO could induce *AOX1a* expression indirectly upon O_3 stress. However, this does not exclude the possibility that NO activates *AOX1a* directly through cADP Rib, which in turn stimulates Ca^{+2} release into the cytoplasm, as happens in PR-1 and PAL activation (Klessig et al., 2000). Furthermore, there is evidence in mammalian system that NO can directly regulate the Ca^{+2} channel via *S*-nitrosylation (Xu et al., 1998) independently of cGMP and cADPR.

In conclusion, under O_3 stress, NO and ET appear to be self-amplifying and cooperate in stimulating the plant response, namely, the AOX pathway. Enhancement of the alternative pathway, in addition to stimulation of the O_3-induced ROS-scavenging enzymes, lowers ROS production and so helps plants to counteract oxidative stress.

MATERIALS AND METHODS

Plant Material

The tobacco (*Nicotiana tabacum* L. cv BelW3) seeds were kindly provided by Dr. V. Sisson of the Oxford Tobacco Research Station (Oxford, NC). Growth chamber conditions were: 14-h photoperiod, photosynthetic photon fluence rate of 120 μmol m^{-2} s^{-1}, day/night air temperature of 25°C/20°C, and relative humidity 60% to 75%. The fourth leaf from the apex of four treated and four untreated (controls) 12-week-old plants were used in all experiments and the experiments were replicated four times.

O_3 Treatment

Plants were exposed for 5 h (8 AM–1 PM) to 150 nL L^{-1} O_3 or to filtered air in plexiglass chambers (0.32 m^3) under light with a photosynthetic photon fluence rate of 400 μmol m^{-2} s^{-1}. The O_3 produced by UV irradiation

(OEG50L lamp; Helios Italquartz s.r.l.) was continuously monitored with a UV-photometric O_3 analyzer (Thermo Electron Corporation). After the O_3 treatment, plants were left in the growth chamber to recover. Leaf injury was determined 48 h after the end of fumigation on the fourth leaf and was scored visually as a percentage of total leaf area, and the data calibrated with a planimeter.

O_3 Uptake Measurement

To determine whether the application of the ET inhibitor AVG, the NO quencher cPTIO, and the NO biosynthesis inhibitor LNNA influenced the O_3 uptake, we measured the actual O_3 influx by leaves exposed to 150 nL L^{-1} O_3 for 5 h in a special gas-exchange instrument. For this purpose we measured the O_3 uptake after 1, 1.5, 2, 2.5, 3, and 5 h of O_3 fumigation in plants painted with water, AVG, or cPTIO + LNNA, as described below, and then fumigated. A 7-cm^2 leaf portion was enclosed in a gas-exchange cuvette and exposed to a flow of 0.5 dm^3 min^{-1} air (80% N_2, 20% O_2, and 350 ppm CO_2). O_3 uptake by the cuvette and other components of the gas-exchange system was minimized by covering exposed surfaces with Teflon film and using Teflon tubing. The gas flow system was constructed as an open system with input and output gas streams continuously measured for CO_2 and water (differential mode; 6262 IR; LI-COR), and O_3 (model 1108; Dasibi Environmental). The leaf temperature was set at 25°C and measured with a copper-constanton thermocouple pressed against the leaf abaxial surface. The relative humidity was set at 40%, and the light intensity was set at 400 μmol m^{-2} s^{-1}. When photosynthesis was stable, the leaf disc was fumigated with 150 nL L^{-1} O_3 for 5 h. A bypass valve was installed to regularly bypass the cuvette and to read the O_3 concentration in the air at the cuvette inlet and outlet. The difference between these two values is the O_3 uptake by the leaf.

Mitochondrial Isolation

Tobacco leaves (50 g fresh weight) were cut and homogenized in a mortar in 120 mL of a medium composed of 20 mM HEPES-Tris, pH 7.6, 0.4 M Suc, 5 mM EDTA, 25 mM potassium metabisulfite, 0.3% (w/v) bovine serum albumin (BSA), and 0.6% (w/v) insoluble polyvinylpolypyrrolidone. The homogenate was then filtered through eight gauze layers. This debris was again homogenized in 100 mL of the medium and filtered once more. The filtrate was centrifuged at 3,500*g* for 5 min at 4°C (first centrifugation). The supernatant was then centrifuged at 28,000*g* for 5 min (second centrifugation). The pellet was resuspended in 120 mL of homogenization medium without polyvinylpolypyrrolidone in a Potter homogenizer. This fraction was centrifuged at 2,500*g* for 3 min (third centrifugation) and the supernatant centrifuged at 28,000*g* for 5 min (fourth centrifugation). The pellet was suspended in 2.5 mL of 10 mM MOPS-KOH, pH 7.2, 0.2 M Suc, and 0.2% (w/v) BSA (suspension buffer), and then purified on a self-forming 32% (v/v) Percoll gradient (Sigma). The mitochondrial band was collected, diluted 25 times with suspension buffer, and centrifuged for 10 min at 10,000*g*. The pellet was suspended in 1 mL of suspension buffer and used for the analyses. The intactness of the outer mitochondrial membrane was monitored by KCN-sensitive, succinate-cyt *c* oxidoreductase activity, as described by Douce et al. (1973), resulting in an intactness from 80% to 90%. The outer mitochondrial integrity was evaluated in mitochondria isolated from unfumigated and fumigated plants, and no significant differences were found in membrane integrity (data not shown). The supernatant obtained after the second centrifugation was centrifuged at 100,000*g* for 40 min and the supernatant fractionated with ammonium sulfate. Solid ammonium sulfate was added at 4°C with stirring to give 40% saturation. The precipitate was removed by centrifugation at 10,000*g* for 10 min and the supernatant brought up to 90% saturation with ammonium sulfate. After 30 min at 4°C, the suspension was centrifuged at 10,000*g* for 10 min. The precipitate, dissolved in 15 mL of 20 mM HEPES-Tris, pH 7.5, and 0.4 M Suc, was dialyzed against 10 mM HEPES-Tris, pH 7.5, for 12 h and represents the cytoplasmic fraction. To assess final mitochondrial contamination, the cytoplasmic fraction was tested for COX activity (Storrie and Madden, 1990) and also examined by western blotting for the presence of COX subunit I. Both analyses demonstrated that no mitochondria were detectable in the cytoplasmic fraction.

Respiratory Measurements

The O_2 uptake by leaf mitochondria isolated from control and O_3-treated plants at 2.5, 5, 10, and 24 h from the start of fumigation was measured in a Clark-type oxygen electrode (YSI 5300A) at 25°C. An aliquot of mitochondrial suspension (approximately 0.2–0.5 mg protein mL^{-1}) was added to the reaction medium containing 10 mM KH_2PO_4, pH 7.2, 0.3 M Suc, 30 mM KCl, 5 mM $MgCl_2$, 0.2 mM ATP, and 0.1% (w/v) BSA (fatty acid-free). Electron transport capacities were measured in the presence of a combination of substrates, consisting of 2 mM NADH, 10 mM succinate, and 0.15 mM ADP. To ensure activation of AOX, 1 mM pyruvate and 10 mM dithiothreitol also were added. Under these assay conditions, respiration rate refers to O_2 uptake in the absence of any addition, while cyt capacity is defined as O_2 uptake that was sensitive to 3 mM KCN in the presence of 1 mM salicylhydroxamic acid (SHAM). AOX capacity is defined as the O_2 uptake that was sensitive to 1 mM SHAM in the presence of 3 mM KCN. Residual respiration (O_2 uptake in the presence of KCN and SHAM) was often not detectable and was assumed equal to zero. The O_2 concentration in air-saturated water at 25°C was assumed to be 230 μM. Mitochondrial protein was determined according to Bradford (1976).

RNA Isolation and Analysis

Total RNA was extracted from frozen, homogenized leaf tissue (0.1–0.15 g fresh weight) of control and O_3-treated plants at 1.5, 2.5, 5, 10, and 24 h from the start of fumigation, using NucleoSpin RNA Plant (Macherey-Nagel) according to the manufacturer's instructions. A given amount of total RNA (1–2 μg) was reverse transcribed for 1 h at 42°C using 200 units of SuperScript II RT (Invitrogen) with 1 × corresponding buffer, 10 mM dithiothreitol, 0.4 mM each dNTP, 0.5 μg oligo$(dT)_{12\text{-}18}$ primer (Invitrogen). The cDNA was used for PCR with 1 unit *Taq* polymerase (Amersham Bioscience), 1 × corresponding buffer, 0.2 mM each dNTP, and 10 μM of the *actin*, *AOX2*, *AOX1a*, *COXI*, *COXII*, and *ACS2* primers (Invitrogen). For analysis of transcripts of AOX, we used the following primers: *AOX2* forward primer 5′-CATCTGAGGTCGTTGCGCAAG-3′ and reverse primer 5′-TTGGGGGACAGCACGTAAAGC-3′ (Norman et al., 2004), and *AOX1a* forward primer 5′-GATGACACGTGGAGCGACAAGG-3′ and reverse primer 5′-CCACTCTGTTCGAATCGCCTAAG-3′. For analysis of other genes, we used the following primers: *ACS2* forward primer 5′-AAGCCTCCATTTGCACAACTG-3′ and reverse primer 5′-GGAAATCCCAAATCTTTCGACAAGC-3′, *COXI* forward primer 5′-GATTGCGATCAAAGTCCATGGTAG-3′ and reverse primer 5′-GCAGCTTCTCCAGAATGGCTGG-3′, and *COXII* forward primer 5′-CTTGTGATGCAGCGGAACCATGGC-3′ and reverse primer 5′-CCGATACCATTGATGTCCAATAGCTT-3′. The cDNA were standardized as reported by Pasqualini et al. (2003). The authenticity of the PCR products was checked by two-directional sequencing using an ABI Prism 310 genetic analyzer (Perkin Elmer Life and Analytical Sciences). For quantification, filters were scanned and band intensities were determined with image-analysis software.

Western Blot and Immunodetection

The proteins from isolated mitochondria (25–150 μg) and the cytoplasmic fraction (100 μg) of control and O_3-treated plants at 1.5, 2.5, 5, 10, and 24 h from the start of fumigation were separated by SDS-PAGE according to Laemmli (1970) and subsequently electrotransferred to nitrocellulose filters. Immunoblot analysis was performed as described previously (Pasqualini et al., 2003). Monoclonal antibodies recognizing AOX (generously supplied by Prof. T. Elthon), COXI and COXII (Molecular Probes), and cyt *c* (Pharmingen) were utilized. Antibodies were used at the following dilutions: AOX 1:100 (v/v), COXI 0.5 μg/mL, COXII 1 μg/mL, and cyt *c* 1:500 (v/v).

Measurement of H_2O_2 in Isolated Mitochondria

The H_2O_2 concentration in mitochondria isolated from control and O_3-treated plants (1.5, 2.5, and 5 h from the start of fumigation) was determined spectrophotometrically by xylenol orange assay as reported previously (Pasqualini et al., 2003).

Visualization of NO

NO accumulation was determined using the fluorescent NO indicator dye DAF-FM diacetate (Molecular Probes). Free-hand leaf sections taken from control (time 0) and O_3-treated plants after 0.5, 1.0, 1.5, 2.0, 2.5, 3.5, and 5 h from the start of fumigation were incubated in the dark for 1 h, at 25°C, with 2 μM DAF-FM prepared in 50 mM Tris-HCl buffer, pH 7.2. Samples were then washed with the probe buffer three times for 15 min, mounted in buffer on

microscope slides, and examined immediately with a UV epifluorescence microscope (DMLB; Leica). Sections were excited with a 450- to 490-nm band-pass filter, and DAF-FM triazole emission was recorded using a 525/20 band-pass filter. To serve as negative controls, sections were incubated in distilled water alone. The incubation of the sections with DAF-FM and 100 μM of the NO scavenger cPTIO (Molecular Probes) eliminated the DA-FM triazole signal. NO detection was also performed in AVG- and cPTIO/LNNA-pretreated plants (see below for methods).

ET Determination

Tobacco leaf segments (approximately 0.3−0.4 g fresh weight) were harvested and placed adaxially into glass tubes (16 mL) that were sealed with silicone septa. After incubation at room temperature for 1 h, 1-mL gas samples were withdrawn with a gas-tight syringe and injected into a gas chromatograph. ET was measured in a gas chromatograph (MEGA SERIES 5300; Carlo Erba Instruments) equipped with a Porapak N (80–100 mesh, 2 m × 2 mm i.d.) column and a flame ionization detector, and linked to a PC with STAR Chromatography software (Varian). Column, injector, and detector temperatures were 70°C, 150°C, and 200°C, respectively.

Elicitor Treatments

To evaluate the role of different elicitors on *AOX* expression, leaf discs (corresponding to 0.15 g fresh weight) were vacuum infiltrated for 3 min with one of the following compounds: 5 mM H_2O_2, 1 mM SA, 160 μM SNP (NO donor), 100 μM JA, 160 μM ferrocyanide, or 160 μM SNP plus 200 μM cPTIO. Water was the control. H_2O_2, SA, SNP, ferrocyanide, and cPTIO were diluted in water. JA was prepared as stock solution of 10 mM in methanol, which was diluted to a final concentration with water. After infiltration, the samples were placed in water for 2 h under light (400 μmol m^{-2} s^{-1}), then frozen in liquid nitrogen and maintained at −80°C until RNA analysis. ET treatment of plants was performed in a plexiglass chamber. A volume of ET was injected into the chamber to give a final concentration of 10 μL L^{-1}. After 2 h, leaf discs were sampled from ET-treated plants, frozen in liquid nitrogen, and maintained at −80°C until RNA analysis.

To elucidate the role of NO in ET synthesis, tobacco leaf pieces (0.3−0.4 g fresh weight) were vacuum-infiltrated with 0.1, 0.5, and 1 mM SNP solutions. The samples were then placed in glass tubes and ET release was measured after 0.5, 1, 1.5, 2, 2.5, 3, 4, 5, 8, 10, and 24 h. For ACS2 transcript analysis, after infiltration with 1 mM SNP, 1 mM ferrocyanide, 1 mM SNP plus 1 mM cPTIO, or water, leaf segments were transferred in distilled water under light (400 μmol m^{-2} s^{-1}) for 1 h, and then frozen in liquid nitrogen and stored at −80°C until mRNA analysis.

To test whether ET can induce NO emission, free-hand leaf sections sampled from plants treated with ET (10 μL L^{-1}) for 2 h were incubated in the dark for 1 h at room temperature in the presence of 2 μM DAF-FM diluted in 50 mM Tris-HCl, pH 7.2. Samples were then washed with the probe buffer three times for 15 min, mounted in buffer on microscope slides, and examined immediately with a UV epifluorescence microscope (DM RHC; Leica). As a control, leaf tissue sampled from plants without ET was incubated with 2 μM DAF-FM. The NO emission in the sections was examined with a UV epifluorescence microscope as described above.

Cyanide Analysis

Leaf discs were infiltrated with 160 μM SNP as above described, and cyanide analysis (Smith and Arteca, 2000) was performed immediately after SNP infiltration (0 h) and after 2, 5, 10, and 24 h.

Measurement of Cell Death

Cell death, indicated as loss of plasma membrane integrity, was measured spectrophotometrically as Evans blue uptake (Baker and Mock, 1994). Leaf tissue (0.4 g fresh weight) was vacuum-infiltrated with 1 mM SNP and then incubated in Evans blue solution (0.25% [w/v] Evans blue in water) for 20 min. After washing for 15 min with water, the trapped Evans blue was released from the leaves by homogenizing leaf tissue with 1.5 mL of 1% (w/v) aqueous SDS. The homogenate was centrifuged at 14,000*g* for 15 min. The optical density of the supernatant was determined at 600 nm. To test the effect of ET inhibition on NO-induced cell death, leaf discs 24 h before SNP infiltration were brushed with 1 mM AVG and Evan blue incorporation evaluated.

Quantification of Endogenous JA and JA Derivatives

According to Hause et al. (2003), with some modifications, fresh plant material (0.5 g) harvested from control and O_3-treated plants at different times (1.5, 2.5, 5, 10, and 24 h, or 20, 40, 60 and 90 min) from the start of fumigation was homogenized with 10 mL of methanol and appropriate nanograms of ($^2H_6$)JA, ($^2H_5$)OPDA, 11-($^2H_3$)OAc-JA, 12-($^2H_3$)OAc-JA, 12-HSO$_4$-JA-($^2H_3$)Me ester, and 12-*O*-($^2H_7$)Gluc-JA as internal standards. The homogenate was filtered, and the eluate was evaporated and acetylated with 200 μL of pyridine and 10 μL of acetic acid anhydride at 20°C overnight. The extract was dried, dissolved in 2 mL of ethyl acetate, and passed through a Chromabond-SiOH column, and the column washed with further 3 mL of ethyl acetate. Combined liquids were evaporated giving Extract A. Further elution with 5 mL of methanol and evaporation of elutes gives Extract B. Extract A: The extract was dissolved with 10 mL of methanol and placed on a column filled with 3 mL of DEAE-Sephadex A-25 (Ac form). The column was washed with 3 mL of methanol. After washing with 3 mL of 0.1 M acetic acid in methanol, the sample, eluted with 3 mL of 1 M acetic acid in methanol and 3 mL of 1.5 M acetic acid in methanol, was collected, evaporated, and separated on preparative HPLC (method 1), derivatizated, and analyzed by gas chromatography-mass spectrometry (GC-MS). Extract B: Sample was methylated with 200 μL of ethereal diazomethane, evaporated, and separated on preparative HPLC (method 2). HPLC: Eurospher 100-C18, 5 μm, 250 × 4 mm (Knauer); solvent A: methanol; solvent B: 0.2% acetic acid in water. Method 1: gradient: 40% A to 100% A in 25 min. The fractions at R_t from 9.75 to 11.75 min (11- and 12-OAc-JA) and 13 to 14.50 min (JA) were collected and evaporated, and 18.50 to 19.50 min (dinor-OPDA) and 21.75 to 22.50 min (OPDA) have to be combined and evaporated. Method 2: gradient 10% A to 100% A in 20 min. Fractions at R_t 9.75 to 11.25 min (12-HSO$_4$-JA-Me) and 17.15 to 18.30 min 12-*O*-tetraacetyl-Glc-JA-Me were collected in 1-mL vial and evaporated. The evaporated samples from method 1 were dissolved in 200 μL of $CHCl_3$/*N*,*N*-diisopropylethylamine (1:1) and derivatized overnight with 10 μL of pentafluorobenzylbromide at 20°C. The evaporated derivatized samples were dissolved in 5 mL of *n*-hexane and passed through a SiOH column (500 mg; Machery-Nagel). The pentafluorobenzyl esters were eluted with 7 mL of *n*-hexane/diethylether (2:1). Elutes were evaporated, dissolved in 100 μL of acetonitrile, and analyzed by GC-MS. The following parameters were used for GC-MS (Finnigan GCQ; Thermo Electron): 70 eV, NCI, ionization gas NH_3, source temperature 140°C, column Rtx-5w (5-m inert precolumn connected with a column 15 m × 0.25 mm, 0.25-μm film thickness; Restek), injection temperature 250°C, interface temperature 275°C; helium 40 cm s^{-1}; splitless injection. Column temperature program was 1 min 60°C, 25°C min^{-1} to 180°C, 5°C min^{-1} to 270°C, 10°C min^{-1} to 300°C, and 10 min 300°C. R_t of pentafluorobenzyl esters: ($^2H_6$)JA 11.80 min, ($^2H_6$)-7-*iso*-JA 12.24 min, JA 11.86 min, 7-*iso*-JA 12.32 min, 11-($^2H_3$)OAc-JA isomer mixture 15.00 to 16.00 min, 11-OAc-JA isomer mixture 15.03 to 16.03 min, 12-($^2H_3$)OAc-JA 17.16 min, 12-($^2H_3$)OAc-7-*iso*-JA 17.63 min, 12-OAc-JA 17.20 min, 12-OAc-7-*iso*-JA 17.66 min, trans-dinor-OPDA 18.47 min, cis-dinor-OPDA 19.14 min, trans-($^2H_5$)OPDA 21.29 min, cis-($^2H_5$)OPDA 21.93 min, trans-OPDA 21.35 min, and cis-OPDA 21.98 min. Fragments *m/z* 209, 215 (standard), *m/z* 267, 270 (standard), *m/z* 267, 270 (standard), *m/z* 263, 296, and *m/z* 291, 296 (standard) were used for the quantification of JA, 11-hydroxyjasmonic acid, 12-hydroxyjasmonic acid, dinor-OPDA, and OPDA, respectively.

The evaporated samples from method 2 were dissolved in 50 μL of methanol and analyzed by LC-MS-MS. The electrospray selected reaction monitoring data were obtained from a Finnigan TSQ 7000 instrument (Thermo Electron; electrospray voltage 4.0 kV; heated capillary temperature 220°C; sheath gas: nitrogen) coupled with a Surveyor MicroLC system equipped with a RP 18-column (4 μm, 1 × 100 mm; Ultrasep). For the HPLC, a gradient system was used starting from H_2O:CH_3CN 90:10 (each of them containing 0.2% HOAc) to 10:90 within 30 min; flow rate 50 μL min^{-1}. 12-HSO$_4$-JA-Me and 12-*O*-tetraacetyl-Glc-JA-Me were determined during one HPLC run by performing the selected reaction monitoring measurements in two different time segments (Software Xcalibur, version 1.3). In segment 1 (0−15 min), the reactions *m/z* 319 ($[M - H]^-$) → *m/z* 97 for 12-HSO$_4$-JA-Me and *m/z* 322 ($[M - H]^-$) → *m/z* 97 for 12-HSO$_4$-JA-($^2H_3$)Me (negative ion mode, collision energy +30 eV), as well as in segment 2 (15–30 min) the reactions *m/z* 571 ($[M + H]^+$) → *m/z* 331 for 12-*O*-tetraacetyl-Glc-JA-Me and *m/z* 578 ($[M + H]^+$) → *m/z* 338 for 12-*O*-tetraacetyl-($^2H_7$)Glc-JA-Me (positive ion mode, collision energy −10 eV), respectively, were measured (collision gas: argon; collision pressure: 1.8 × 10^{-3} Torr). The measured peak areas were used for the quantification of 12-HSO$_4$-JA-Me and 12-*O*-tetraacetyl-Glc-JA-Me.

ET Inhibition Treatment

The inhibitor of ET biosynthesis, AVG (Sigma), at a concentration of 1 mM, was applied 24 h before O_3 treatment by brushing it onto the adaxial surface of the leaves. As a control, plants were painted with water. Leaf samples (0.5 g fresh weight) were taken before the start of fumigation and from O_3-treated and untreated plants after 1, 2, 5, 10, and 24 h for ET determination. AVG-treated plants were also analyzed for NO accumulation as described above.

NO Inhibition Treatment

The inhibitor of NOS, LNNA (Sigma), at a concentration of 10 mM, was applied 24 h before O_3 treatment by brushing it onto the adaxial surface of the leaves. At 1.5 h before O_3 fumigation started, the leaves were painted with 200 μM of the NO scavenger cPTIO. As a control, plants were painted with water. The treatment with cPTIO was repeated three times during fumigation. Samples of leaf (0.5 g fresh weight) were taken from O_3-treated and untreated plants after 1, 2, and 5 h for ACS2 transcript analysis, and also after 10 and 24 h for ET determination. LNNA/cPTIO-treated plants were also examined for NO accumulation as described above.

Statistical Analysis

Each treatment was replicated four times. The means ± SE are shown in Figures 1, 2, 4, 5, 6, 7, and 8 and in Supplemental Figures S1 to S4. In Figure 4 and Supplemental Figures S1, S2C, S3, and S4, the values followed by different letters are significantly different at $P \leq 0.01$, whereas in Figure 6 were at $P \leq 0.05$ (ANOVA).

Sequence data from this article can be found in the NCBI/GenBank data libraries under the following accession numbers: S711335 (*AOX1a*), AJ005002 (*ACS2*), AY237826 (*COXI*), and BAD83476 (*COXII*).

Supplemental Data

The following materials are available in the online version of this article.

Supplemental Figure S1. Leaf discs were infiltrated with 160 μM SNP, and cyanide concentration detected immediately after infiltration (0 h) and after 2, 5, 10, and 24 h.

Supplemental Figure S2. Content of JA and JA derivatives determined by GC-MS analysis.

Supplemental Figure S3. Effect of SNP and SNP + cPTIO on purified mitochondria.

Supplemental Figure S4. Endogenous H_2O_2 accumulation in leaf discs infiltrated with 5 mM H_2O_2.

ACKNOWLEDGMENT

We thank Judy Etherington for her invaluable help in the English editing of the manuscript.

Received June 20, 2006; accepted August 11, 2006; published August 25, 2006.

LITERATURE CITED

Affourtit C, Albury MSW, Crichton PG, Moore AL (2002) Exploring the molecular nature of alternative oxidase regulation and catalysis. FEBS Lett **510:** 121–126

Atkin OK, Zhang QS, Wiskich JT (2002) Effect of temperature on rates of alternative and cytochrome pathway respiration and their relationship with the redox poise of the quinone pool. Plant Physiol **128:** 212–222

Baker CJ, Mock NM (1994) An improved method for monitoring cell death in cell suspension and leaf disc assays using evans blue. Plant Cell Tissue Organ Cult **39:** 7–12

Beligni MV, Lamattina L (2000) Nitric oxide stimulates seed germination and de-etiolation and inhibits hypocotyl elongation, three light-inducible responses in plants. Planta **210:** 215–221

Bentke PC, Libourel IGL, Reinol V, Jones RL (2006) Sodium nitroprusside, cyanide, nitrite, and nitrate break *Arabidopsis* seed dormancy in a nitric oxide-dependent manner. Planta **223:** 805–812

Bradford M (1976) A rapid and sensitive method for the quantitation of microgram quantities of protein utilizing the principle of protein-dye binding. Anal Biochem **72:** 248–254

Braidot E, Petrussa E, Vianello A, Macri F (1999) Hydrogen peroxide generation by higher plant mitochondria oxidizing complex I or complex II substrates. FEBS Lett **451:** 347–350

Chivasa S, Carr JP (1998) Cyanide restores N gene-mediated resistance to tobacco mosaic virus in transgenic tobacco expressing salicylic acid hydroxylase. Plant Cell **10:** 1489–1498

Clarke A, Desikan R, Hurst RD, Hancock JT, Neil SJ (2000) NO way back: nitric oxide and programmed cell death in *Arabidopsis thaliana* suspension cultures. Plant J **24:** 667–677

Delledonne M, Xia YJ, Dixon RA, Lamb C (1998) Nitric oxide functions as a signal in plant disease resistance. Nature **394:** 585–588

Djajanegara I, Finnegan PM, Mathieu C, McCabe T, Whelan J, Day DA (2002) Regulation of alternative oxidase gene expression in soybean. Plant Mol Biol **50:** 735–742

Douce R, Christensen E, Bonner WD Jr (1973) The external NADH deydrogenases of intact plant mitochondria. Biochim Biophys Acta **292:** 105–116

Durner J, Wendehenne D, Klessig DF (1998) Defense gene induction in tobacco by nitric oxide, cyclic GMP, and cyclic ADP-ribose. Proc Natl Acad Sci USA **95:** 10328–10333

Dutilleul C, Garmier M, Noctor G, Mathieu C, Chetrit P, Foyer CH, de Paepe R (2003) Leaf mitochondria modulate whole cell redox homeostasis, set antioxidant capacity, and determine stress resistance through altered signaling and diurnal regulation. Plant Cell **15:** 1212–1226

Fung RWM, Wang CY, Smith DL, Gross KC, Tian MS (2004) MeSA and MeJA increase steady-state transcript levels of alternative oxidase and resistance against chilling injury in sweet peppers (*Capsicum annuum* L.). Plant Sci **166:** 711–719

Garcia-Mata C, Lamattina L (2002) Nitric oxide and abscisic acid cross talk in guard cells. Plant Physiol **128:** 790–792

Gidda SK, Miersch O, Levitin A, Schimdt J, Wasternack C, Varin L (2003) Biochemical and molecular characterization of a hydroxyjasmonate sulfotransferase from *Arabidopsis thaliana*. J Biol Chem **278:** 17895–17900

Gould KS, Lamotte O, Klinguer A, Pugin A, Wendehenne D (2003) Nitric oxide production in tobacco leaf cells: a generalized stress response? Plant Cell Environ **26:** 1851–1862

Halliwell B, Gutteridge JMC (1999) Free Radicals in Biology and Medicine. Oxford University Press, New York

Hause B, Stenzel I, Miersch O, Wasternack C (2003) Occurrence of allene oxide cyclase in different organs and tissues of *Arabidopsis thaliana*. Phytochemistry **64:** 971–980

Heggestad HE (1991) Origin of Bel-W3, Bel-C and Bel-B tobacco varieties and their use as indicators of ozone. Environ Pollut **74:** 264–291

Huang X, von Rad U, Durner J (2002) Nitric oxide induces transcriptional activation of the nitric oxide-tolerant alternative oxidase in *Arabidopsis* suspension cells. Planta **215:** 914–923

Jones A (2000) Does the plant mitochondrion integrate cellular stress and regulate programmed cell death? Trends Plant Sci **5:** 225–230

Joo JH, Wang S, Chen JG, Jones AM, Fedoroff NV (2005) Different signaling and cell death roles of heterotrimeric G protein α and β subunits in the Arabidopsis oxidative stress responses to ozone. Plant Cell **17:** 957–970

Kangasjärvi J, Jaspers P, Kollist H (2005) Signalling and cell death in ozone-exposed plants. Plant Cell Environ **28:** 1021–1036

Klessig DF, Durner J, Noad R, Navarre DA, Wendehenne D, Kumar D, Zhou JM, Shah J, Zhang SQ, Kachroo P, et al (2000) Nitric oxide and salicylic acid signaling in plant defense. Proc Natl Acad Sci USA **97:** 8849–8855

Koch JR, Creelman RA, Eshita SM, Seskar M, Mullet JE, Davis KR (2000) Ozone sensitivity in hybrid poplar correlates with insensitivity to both salicylic acid and jasmonic acid. The role of programmed cell death in lesion formation. Plant Physiol **123:** 487–496

Kojima H, Nakatsubo N, Kikuchi K, Kawaahara S, Kirino Y, Nagoshi H, Hirata Y, Nagano T (1998) Detection and imaging of nitric oxide with novel fluorescent indicators: diaminofluoresceins. Anal Chem **70:** 2446–2453

Kroemer G (1997) Mitochondrial implication in apoptosis. Towards an endosymbiont hypothesis of apoptosis evolution. Cell Death Differ **4:** 443–456

Laemmli UK (1970) Cleavage of structural proteins during the assembly of the head of bacteriophage. Nature **227:** 680–685

Lam E, Kato N, Lawton M (2001) Programmed cell death, mitochondria and the plant hypersensitive response. Nature **411:** 848–853

Lambers H, Steingrover E (1978) Efficiency of root respiration of a flood-tolerant and a flood-intolerant *Senecio* species as affected by low oxygen tension. Physiol Plant **42:** 179–184

Langebartels C, Kerner K, Leonardi S, Schraudner M, Trost M, Heller W, Sandermann H (1991) Biochemical plant responses to ozone. 1. Differential induction of polyamine and ethylene biosynthesis in tobacco. Plant Physiol **95:** 882–889

Lennon AM, Neuenschwander UH, Ribas-Carbo M, Giles L, Ryals JA, Siedow JN (1997) The effect of salicylic acid and tobacco mosaic virus infection on the alternative oxidase of tobacco. Plant Physiol **115:** 783–791

Liao XS, Butow RA (1993) RTG1 and RTG2: two yeast genes required for a novel path of communication from mitochondria to the nucleus. Cell **72:** 61–71

Maxwell DP, Nickels R, McIntosh L (2002) Evidence of mitochondrial involvement in the transduction of signals required for the induction of genes associated with pathogen attack and senescence. Plant J **29:** 269–279

Maxwell DP, Wang Y, McIntosh L (1999) The alternative oxidase lowers mitochondrial reactive oxygen production in plant cultures. Proc Natl Acad Sci USA **96:** 8271–8276

McDonald AE, Sieger SM, Vanlerberghe GC (2002) Methods and approaches to study plant mitochondrial alternative oxidase. Physiol Plant **116:** 135–143

Millar AH, Day DA (1996) Nitric oxide inhibits the cytochrome oxidase but not the alternative oxidase of plant mitochondria. FEBS Lett **398:** 155–158

Millar AH, Day DA (1997) Alternative solutions to radical problems. Trends Plant Sci **2:** 289–290

Millenaar FF, Gonzales-Meler MA, Fiorani F, Welschen R, Ribas-Carbo M, Siedow J, Wagner AM, Lambers H (2001) Regulation of alternative oxidase activity in six wild monocotyledonous species. An in vivo study at the whole root level. Plant Physiol **126:** 376–387

Millenaar FF, Lambers H (2003) The alternative oxidase: in vivo regulation and function. Plant Biol **5:** 2–15

Minagawa N, Koga S, Nakano M, Sakajo S, Yoshimoto A (1992) Possible involvement of superoxide anion in the induction of cyanide-resistant respiration in *Hansenula-anomala.* FEBS Lett **302:** 217–219

Neill SJ, Desikan R, Clarke A, Hancock JT (2002) Nitric oxide is a novel component of abscisic acid signalling in stomatal guard cells. Plant Physiol **128:** 13–16

Norman C, Howell KA, Millar AH, Whelan JM, Day DA (2004) Salicylic acid is an uncoupler and inhibitor of mitochondrial electron transport. Plant Physiol **134:** 492–501

Örvar BL, McPherson J, Ellis BE (1997) Pre-activating wounding response in tobacco prior to high-level ozone exposure prevents necrotic injury. Plant J **11:** 203–212

Overmyer K, Broscé M, Kangasjärvi J (2003) Reactive oxygen species and hormonal control of cell death. Trends Plant Sci **7:** 335–342

Overmyer K, Brosché M, Pellinen R, Kuittinen T, Tuominen H, Ahlfors R, Keinanen M, Saarma M, Scheel D, Kangasjärvi J (2005) Ozone-induced programmed cell death in the Arabidopsis radical-induced cell death1 mutant. Plant Physiol **137:** 1092–1104

Parani M, Rudrabhatla S, Myers R, Weirich H, Smith B, Leaman DW, Goldman SL (2004) Microarray analysis of nitric oxide responsive transcripts in *Arabidopsis.* Plant Biotechnol J **2:** 359–366

Pasqualini S, Della Torre G, Ferranti F, Ederli L, Piccioni C, Reale L, Antonielli M (2002) Salicylic acid modulates ozone-induced hypersensitive cell death in tobacco plants. Physiol Plant **115:** 204–212

Pasqualini S, Piccioni C, Reale L, Ederli L, Della Torre G, Ferranti F (2003) Ozone-induced cell death in tobacco cultivar BelW3 plants. The role of programmed cell death in lesion formation. Plant Physiol **133:** 1122–1134

Polidoros AN, Mylona PV, Pasentsis K, Scandalios JG, Tsaftais A (2005) The maize alternative oxidase 1a (*Aox1a*) gene is regulated by signals related to oxidative stress. Redox Rep **10:** 71–78

Poyton RO, McEwen JE (1996) Crosstalk between nuclear and mitochondrial genomes. Annu Rev Biochem **65:** 563–607

Purvis AC (1997) Role of alternative oxidase in limiting superoxide production by plant mitochondria. Physiol Plant **100:** 165–170

Purvis AC, Shewfelt RL (1993) Does the alternative pathway ameliorate chilling injury in sensitive plant tissue? Physiol Plant **88:** 712–718

Rao MV, Davis KR (1999) Ozone-induced cell death occurs via two distinct mechanisms in *Arabidopsis*: the role of salicylic acid. Plant J **17:** 603–614

Rao MV, Davis KR (2001) The physiology of ozone induced cell death. Planta **213:** 682–690

Rao MV, Lee H, Creelman RA, Mullet JE, Davis KR (2000) Jasmonic acid signaling modulates ozone-induced hypersensitive cell death. Plant Cell **12:** 1633–1646

Rhoads DM, McIntosh L (1993) Cytochrome and alternative pathway respiration in tobacco. Effects of salicylic acid. Plant Physiol **103:** 877–883

Sabar M, De Paepe R, Kouchkovsky Y (2000) Complex I impairment, respiratory compensations, and photosynthetic decrease in nuclear and mitochondrial male sterile mutants of *Nicotiana sylvestris.* Plant Physiol **124:** 1239–1249

Schraudner M, Moeder W, Wiese C, Van Camp W, Inze D, Langebartels C, Sandermann H (1998) Ozone-induced oxidative burst in the ozone biomonitor plant, tobacco Bel W3. Plant J **16:** 235–245

Sharma YK, Leon J, Raskin I, Davis KR (1996) Ozone-induced responses in *Arabidopsis thaliana*: the role of salicylic acid in the accumulation of defense-related transcripts and induced resistance. Proc Natl Acad Sci USA **93:** 5099–5104

Simons BH, Millenaar FF, Mulder L, Van Loon LC, Lambers H (1999) Enhanced expression and activation of the alternative oxidase during infection of Arabidopsis with *Pseudomonas syringae* pv tomato. Plant Physiol **120:** 529–538

Smith JM, Arteca RN (2000) Molecular control of ethylene production by cyanide in *Arabidopsis thaliana.* Physiol Plant **109:** 180–187

Storrie B, Madden EA (1990) Isolation of subcellular organelles. Methods Enzymol **182:** 203–235

Tosti N, Pasqualini S, Borgogni A, Ederli E, Falistocco E, Crisp S, Paolocci F (2006) Gene expression profiles of ozone-treated *Arabidopsis* plants. Plant Cell Environ **29:** 1686–1702

Tuomainen J, Betz C, Kangasjärvi J, Ernst D, Yin ZH, Langebartels C, Sandermann H (1997) Ozone induction of ethylene emission in tomato plants: regulation by differential accumulation of transcripts for the biosynthetic enzymes. Plant J **12:** 1151–1162

Tuominen H, Overmyer K, Keinanen M, Kollist H, Kangasjärvi J (2004) Mutual antagonism of ethylene and jasmonic acid regulates ozone-induced spreading cell death in *Arabidopsis.* Plant J **39:** 59–68

Vanlerberghe GC, McIntosh L (1994) Mitochondrial electron transport regulation of nuclear gene expression: studies with the alternative oxidase gene of tobacco. Plant Physiol **105:** 867–874

Vanlerberghe GC, McIntosh L (1996) Signals regulating the expression of the nuclear gene encoding alternative oxidase of plant mitochondria. Plant Physiol **111:** 589–595

Vanlerberghe GC, McIntosh L (1997) Alternative oxidase: from gene to function. Annu Rev Plant Physiol Plant Mol Biol **48:** 703–734

Vanlerberghe GC, McIntosh L, Yip JH (1998) Molecular localization of a redox-modulated process regulating plant mitochondrial electron transport. Plant Cell **10:** 1551–1560

Vanlerberghe GC, Robson CA, Yip JYH (2002) Induction of mitochondrial alternative oxidase in response to a cell signal pathway down-regulating the cytochrome pathway prevents programmed cell death. Plant Physiol **129:** 1829–1842

Vanlerberghe GC, Vanlerberghe AE, McIntosh L (1997) Molecular genetic evidence of the ability of alternative oxidase to support respiratory carbon metabolism. Plant Physiol **113:** 657–661

Velikova V, Pinelli P, Pasqualini S, Reale L, Ferranti F, Loreto F (2005) Isoprene decreases the concentration of nitric oxide in leaves exposed to elevated ozone. New Phytol **166:** 419–426

Wagner AM, Krab K (1995) The alternative respiration pathway in plants: role and regulation. Physiol Plant **95:** 318–325

Whelan J, Millar AH, Day DA (1996) The alternative oxidase is encoded in a multigene family in soybean. Planta **198:** 197–201

Xu L, Eu JP, Meissner G, Stamler JS (1998) Activation of the cardiac calcium release channel (ryanodine receptor) by poly-S-nitrosylation. Science **279:** 234–237

Yip JYH, Vanlerberghe GC (2001) Mitochondrial alternative oxidase acts to dampen the generation of active oxygen species during a period of rapid respiration induced to support a high rate of nutrient uptake. Physiol Plant **112:** 327–333

Zottini M, Formentin E, Scattolin M, Carimi F, Lo Schiavo F, Terzi M (2002) Nitric oxide affects plant mitochondrial functionality in vivo. FEBS Lett **515:** 75–78